ACS Energy LETTERS

http://pubs.acs.org/journal/aelccp

Rapid, Direct Regeneration of Spent $LiCoO_2$ Cathodes for Li-Ion Batteries

Yun-Chao Yin,[#] Chao Li,[#] Xueshan Hu, Daxian Zuo, Lin Yang, Lihui Zhou, Jinlong Yang, and Jiayu Wan*

Cite This: *ACS Energy Lett.* 2023, 8, 3005−3012

Read Online

ACCESS | Metrics & More | Article Recommendations | Supporting Information

ABSTRACT: Recycling of spent lithium-ion batteries is essential for the sustainable development of renewable energy technologies, as it promotes resource reuse and environmental protection. Recycling cathode materials is particularly important due to their high concentration of strategic elements. However, traditional recycling methods for cathode materials are often inefficient due to high energy consumption and prolonged operation time. Here, we present an efficient, one-step, nondestructive method for regenerating spent $LiCoO_2$ cathodes within seconds. This method simultaneously achieves relithiation of the cathode material and repair of the crystal structure through rapid Joule heating. Compared to traditional repair methods, this process exhibits low energy consumption and shortened operation time. After an 8 s repair process, the regenerated $LiCoO_2$ has a well-defined layered structure and is restored to its original electrochemical performance, with an initial discharge capacity of 133.0 mAh/g and good cycling performance. This work represents a potentially universal approach for the efficient direct regeneration of cathode materials.

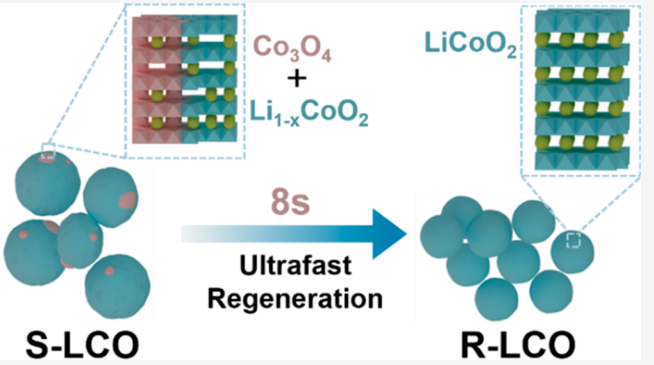

The use of lithium-ion batteries (LIBs) as a sustainable and efficient energy storage device has diffused ubiquitously in recent times, primarily in the consumer electronics, electric vehicle (EV), and grid storage sectors, in support of carbon neutrality goals.[1−6] The global demand for lithium-ion batteries (LIBs) is expected to exceed hundreds of gigawatt hours per year over the next five years, accounting for 70% of the rechargeable battery market by 2025.[7−9] The average lifetime of rechargeable LIBs is no more than three years for portable electronics and five to ten years for EVs, resulting in a significant number of degraded batteries in the near future.[10,11] These spent batteries contain harmful substances such as heavy metals and toxic organic compounds, which pose a risk to the environment and human health.[12−14] On the other hand, the metallic resources used to synthesize cathode materials are becoming increasingly scarce, and the their soaring price in recent years suggests that the future demand is approaching the identified reserves.[15,16] Therefore, it is urgent to develop effective methods for dealing with spent batteries to prevent negative impacts on the environment and to meet the demand for valuable resources, particularly in the era of increased transport electrification and grid-scale storage.

Currently, recycling methods for cathode materials are primarily divided into metallurgical processes (such as pyrometallurgy and hydrometallurgy) and direct repair processes.[17−19] Although metallurgy has been utilized for a long time, it is associated with several drawbacks. For example, hydrometallurgical processes require large amounts of acid to dissolve metal ions in the cathode materials, resulting in the subsequent treatment of large volumes of wastewater.[20,21] The pyrometallurgical process, which is used to obtain valuable metals such as Co, also requires high temperatures and energy to smelt the cathode materials. These metallurgical-based recycling processes involve the destruction of spent cathode materials, metal extraction and purification, and the synthesis of new cathode materials.[22−24] As a result, they are multistep, energy-intensive, and time-consuming. In recent years, there has been a growing interest in developing methods for the direct regeneration of cathode materials without destroying their crystal structure.[25−28] Several methods have been developed, including solid-state sintering,[29,30] molten salt method,[31−33] chemical lithiation strategy,[34−36] hydrothermal method,[37−39] and *in situ* electrochemical method.[40,41] For

Received: March 24, 2023
Accepted: May 26, 2023
Published: June 14, 2023

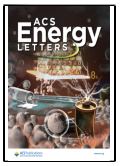

https://doi.org/10.1021/acsenergylett.3c00635
ACS Energy Lett. 2023, 8, 3005−3012

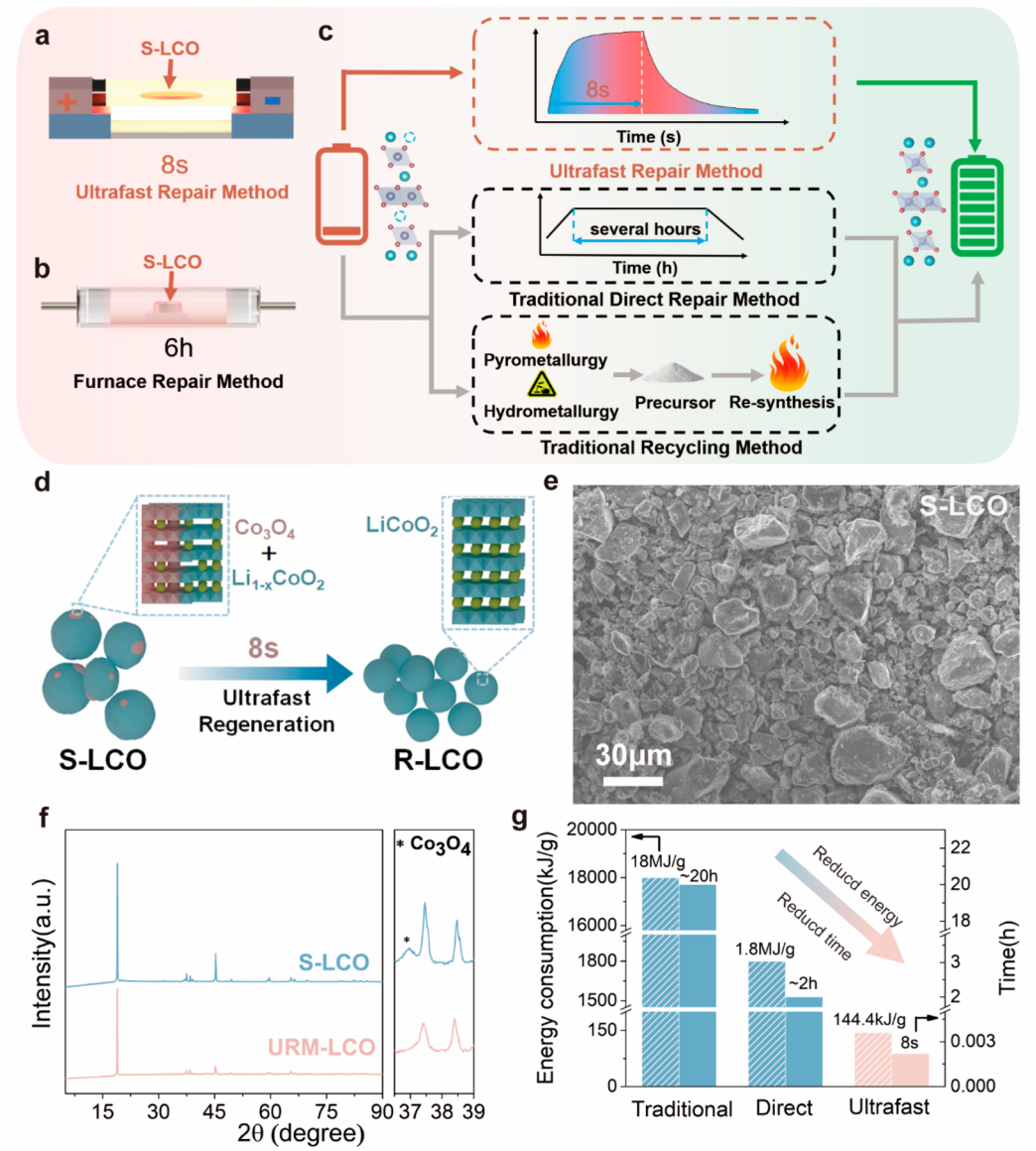

Figure 1. Schematic of (a) the ultrafast repair process and (b) furnace repair method; (c) schematic of the regeneration process; (d) schematic of the repair process of S-LCO; (e) SEM image of S-LCO; (f) XRD patterns of spent $LiCoO_2$ and URM-LCO; (g) energy consumption and operation times of different regeneration processes.

example, Zhang et al. reported that degraded $LiCoO_2$ (LCO) can be regenerated by a solid-state sintering approach in air using Li_2CO_3 as the Li source at 900 °C for 12 h.[29] The electrochemical properties of the regenerated cathode are comparable to those of fresh materials. Zhou et al. reported that spent $LiCoO_2$ (S-LCO) can be regenerated by annealing them at 850 °C in air for 2 h after the relithiation in lithium-containing eutectic solvent, where the phase structure and electrochemical performance of cathode materials are completely recovered.[33] However, all of the aforementioned methods require prolonged high-temperature processes to repair the crystal structure of the cathode material, resulting in relatively long time and high energy consumption requirements. Therefore, a rapid and highly effective method for efficiently regenerating cathode materials is still in high demand.

To achieve highly energy- and time-efficient cathode material regeneration, we propose a nondestructive, ultrafast method for the regeneration of spent LCO in seconds, as illustrated in Figure 1a. Compared with the traditional metallurgical processes and direct repair process based on furnace heating (Figure 1b), the ultrafast repair method (URM) utilizes Joule heating with high heating rate, adjustable temperature, and high cooling rate, which can considerably reduce the unavoidable heat dissipation.[42−46] Notably, the reaction temperature of the URM is relatively higher than that of other traditional recycling methods, allowing the S-LCO to be rapidly repaired within 8 s. The rapid process not only minimizes the loss of the lithium source at high temperature but also avoids the melting and possible corrosive reaction between the lithium source and the container. Our characterization results indicate that the bulk crystal structure of degraded cathodes can be fully recovered despite the rapid process, where the spinel Co_3O_4 formed during long-term cycling is converted to the desired layered structure of LCO. Additionally, the electrochemical performance of the regenerated LCO is comparable to that of fresh commercial cathode materials. Our results suggest that the URM is highly time- and

https://doi.org/10.1021/acsenergylett.3c00635
ACS Energy Lett. 2023, 8, 3005−3012

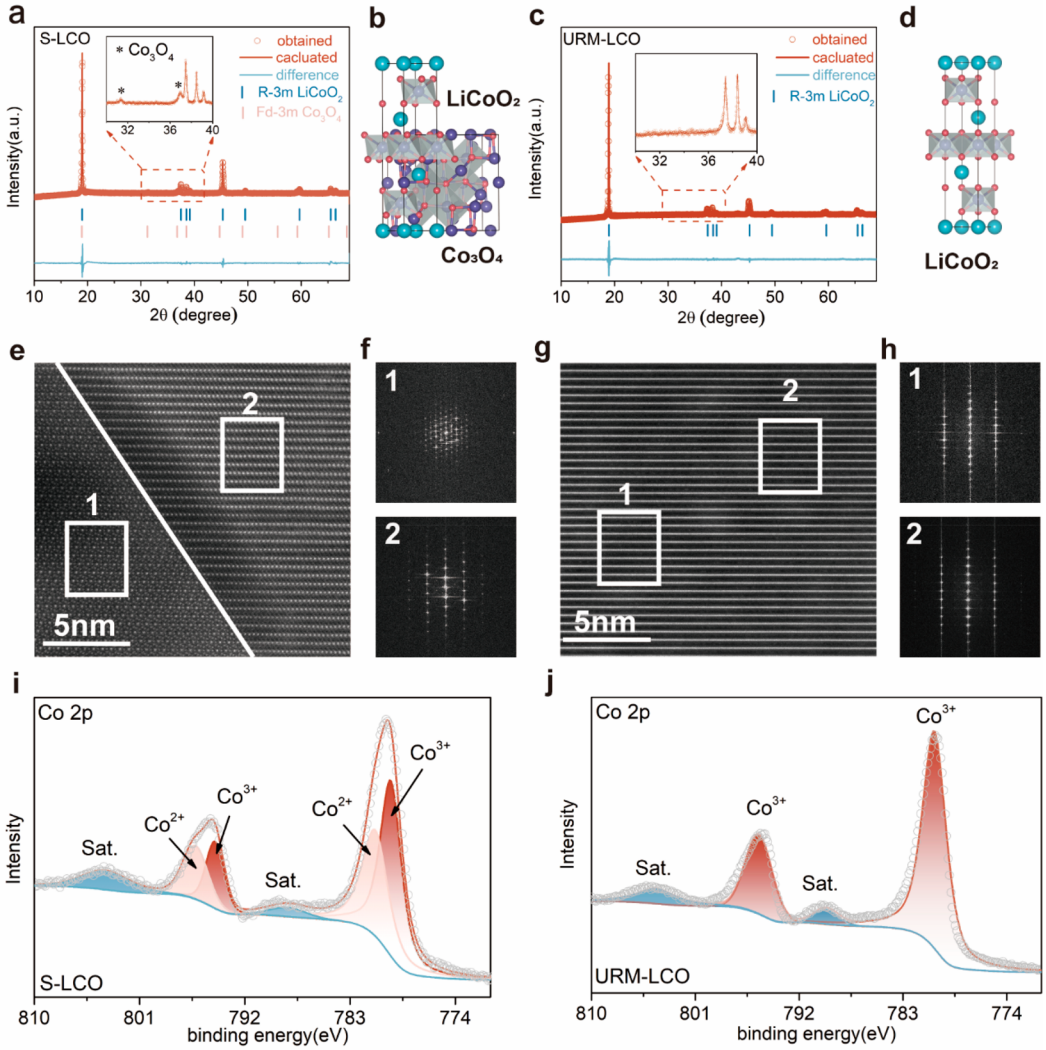

Figure 2. (a) XRD Rietveld refinement results for S-LCO; (b) crystal structures of S-LCO; (c) Rietveld refinement of URM-LCO; (d) crystal models of URM-LCO; (e) HAADF-STEM image of S-LCO; (f) corresponding FFT pattern of the marked region in panel e; (g) HAADF-STEM image of URM-LCO; (f) corresponding FFT pattern of the region marked in panel g; high-resolution XPS spectra of the Co 2p for (i) S-LCO and (j) URM-LCO.

energy-efficient and can simultaneously relithiate the spent cathode materials while repairing their crystal structure. The proposed method demonstrates a highly effective and potentially universal approach in regeneration of battery cathodes.

During the repair and resynthesis of spent cathode materials, a high temperature treatment is usually required. In a typical URM process, pressed pellet samples with a diameter of 1.0 cm are placed between two sheets of carbon paper. The carbon papers and samples are then heated rapidly through Joule heating (Figure 1a), avoiding the prolonged low-temperature reaction stage of furnace-based methods (Figure 1b). Compared with other cathode regenerating methods (Figure 1c), the URM can complete the reaction in a few seconds, effectively reducing unnecessary energy consumption and operating time. Figure 1d illustrates the microscopic repair process of S-LCO, which consists of two major steps. First, the added lithium source fills the lithium vacancy, thereby enabling the reintroduction of lithium ions into the cathode structure. Second, the spinel Co_3O_4 is converted into layered LCO. The highly adjustable nature of URM enables the appropriate reaction temperature for regenerating the cathode within several seconds, avoiding volatilization of lithium at prolonged high temperatures or incomplete crystal phase repair at low reaction temperatures. The SEM image of the S-LCO (Figures 1e and S1) collected from spent commercial LIBs reveals nonuniform particle size and rough surface, where its X-ray diffraction (XRD) result (Figure 1f) shows the coexistence of spinel Co_3O_4 and layered LCO, consistent with previous reports.[29] After URM (at around 1440 K and 8 s treatment), the peak of Co_3O_4 disappeared, indicating the successful structural repair of S-LCO. We then compare the energy and time consumption of URM and conventional recycling methods. The energy consumption is calculated from the amount of electrical power used during the cathode materials' repairing process. As illustrated in Figure 1g, the URM process exhibits significantly less operating time and energy consumption among various methods.

We carried out several materials characterizations, such as XRD, transmission electron microscopy (TEM), and X-ray photoelectron spectroscopy (XPS), to further confirm the effectiveness of URM for LCO regeneration. To begin with, we

https://doi.org/10.1021/acsenergylett.3c00635
ACS Energy Lett. 2023, 8, 3005−3012

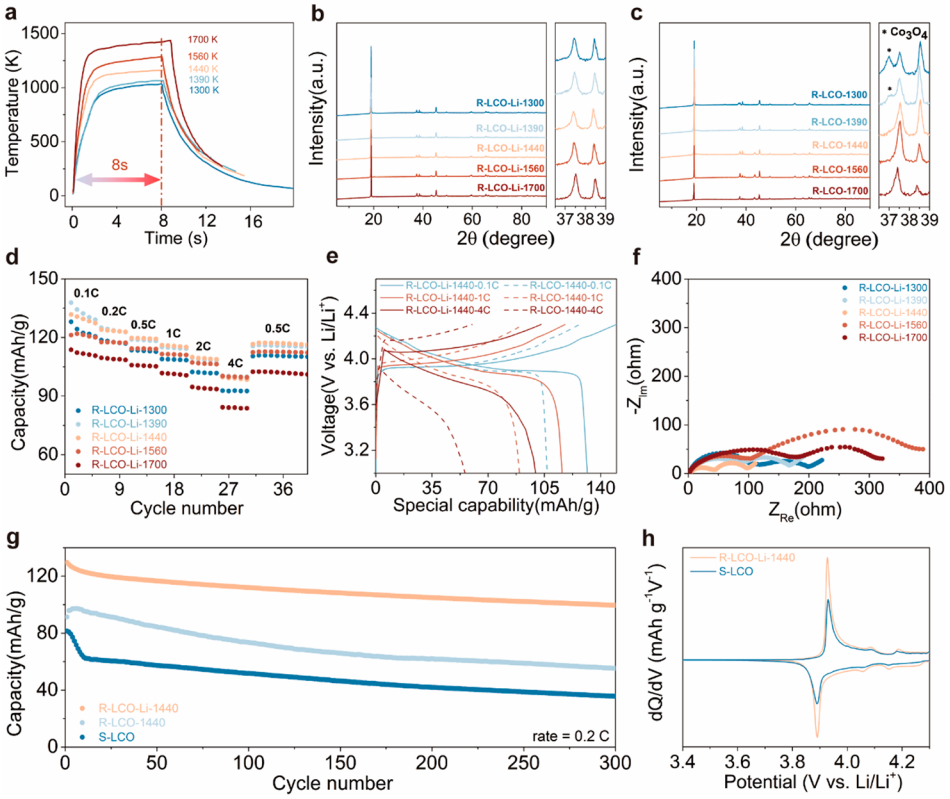

Figure 3. (a) Temperature evolution during the experiment; (b) XRD patterns of the R-LCO with the Li_2CO_3 as Li source under different temperature; (c) XRD patterns of the regenerated $LiCO_2$ without Li source under different temperature; (d) rate performance of the R-LCO with the Li_2CO_3 as Li source under different temperature; (e) charge−discharge curves of R-LCO-Li-1440 (solid line) and R-LCO-1440 (dotted line) under different current; (f) EIS curves of the R-LCO-Li-T; (g) cycling performance of S-LCO, R-LCO-Li-1440, and R-LCO-Li-1440 at 0.2 C; (h) d*Q*/d*V* curve of S-LCO and R-LCO-Li-1440.

performed refined XRD analysis on both the S-LCO and the LCO regenerated by URM with Li_2CO_3 as Li source at 1440 K (URM-LCO). As shown in Figure 2a, the existence of the peaks at 31.34° and 36.96° from the S-LCO sample indicates the presence of spinel Co_3O_4. Other peaks in the S-LCO match well with the hexagonal $R\bar{3}m$ structure. The content of spinel Co_3O_4 was determined to be 2.606 wt % by the Rietveld refined process (Table S1), and the corresponding atomic model of S-LCO is shown in Figure 2b. In contrast, the XRD patterns of URM-LCO only show an identical layered oxide structure with $R\bar{3}m$ space group after the URM process (Figure 2c). The Rietveld refined results showed that the cell parameters of URM-LCO were similar to those of commercial $LiCoO_2$, which is slightly smaller than that of S-LCO (Table S1). These results indicate the microstructure and phase structure of S-LCO can be completely repaired after the ultrafast treatment (Figure 2d). Atomic resolution TEM characterizations were then carried out to verify the above analysis. The high-angle annular dark-field scanning transmission electron microscopy (HAADF-STEM) images of S-LCO at different magnifications and regions exhibit the coexistence of spinel phase and layered structure (Figures 2e and S2), which was verified by the corresponding fast Fourier transform (FFT) (Figure 2f). Notably, the cobalt atomic layer in S-LCO exhibits some degree of distortion. These observations indicate that the microstructure of LCO experiences partial collapse after long-term cycling processes (Figure S2). The highly resolved elemental mapping result demonstrated the homogeneous distribution of Co and O and the existent of the impure phase (Figure S3). The lattice spacing of the corresponding layered structure in S-LCO was 0.486 nm, which corresponds to the (003) peak (Figure S4).

After the URM process, the SEM image showed that the URM-LCO obtained a uniform particle size and a smooth surface (Figure S5). Additionally, only an ordered layer structure was observed in URM-LCO (Figures 2g and S6), which was confirmed by the FFT corresponding to different positions in the STEM-HAADF image of URM-LCO (Figure 2h). Moreover, the distortion in the cobalt atomic layer has been rectified with remarkable precision (Figure S6). A homogeneous distribution of Co and O atoms is observed in highly resolved elemental mapping results of the R-LCO sample (Figure S7), and its (003) crystal plane spacing was measured to be 0.48 nm (Figure S8). All the above observations suggest that this method can efficiently repair the microstructure of S-LCO. The chemical states of Co element in the samples were explored by XPS. The Co 2p spectrum of S-LCO exhibited two prominent peaks, with a peak difference of approximately 15.0 eV, demonstrating the existence of both Co^{2+} and Co^{3+} (Figure 2i).[47] The binding energy of Co 2p at 780.9 and 796.3 eV corresponds to the Co^{2+}, while 780.3 and 794.6 eV correspond to the Co^{3+}.[48] In contrast, we only observed the peaks corresponding to Co^{3+} in the URM-LCO result, manifesting the URM process could regenerate the LCO cathode (Figure 2j). The XPS O 1s spectrum of S-LCO and URM-LCO was deconvoluted into two components corresponding to the lattice oxygen and O=C−O (Figure S9).[48] The intensity peak of lattice oxygen in

https://doi.org/10.1021/acsenergylett.3c00635
ACS Energy Lett. 2023, 8, 3005−3012

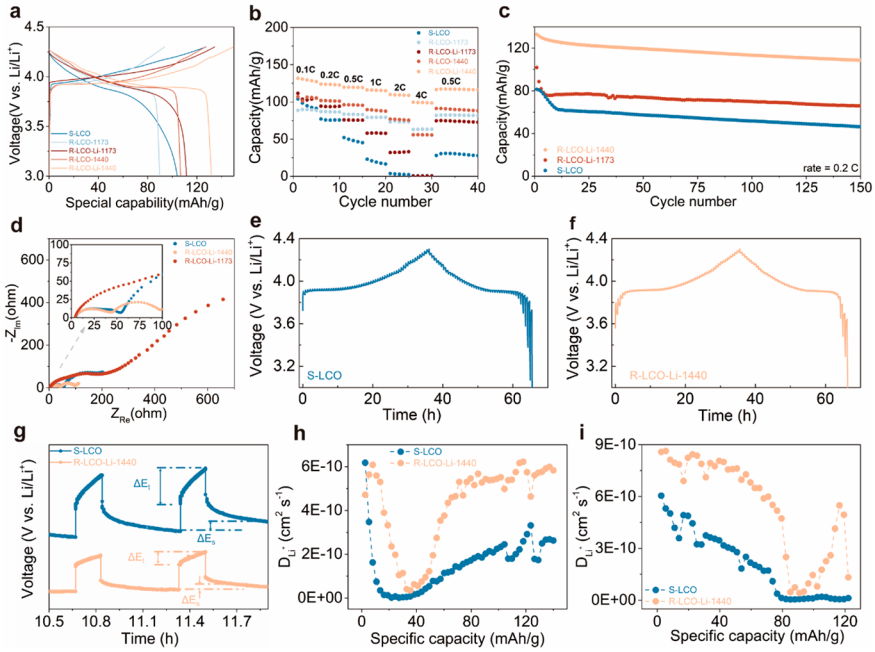

Figure 4. (a) Charge−discharge curves of S-LCO, R-LCO-1173, R-LCO-Li-1173, R-LCO-1440, and R-LCO-Li-1440; (b) rate performance of different samples; (c) long-term performance of the S-LCO, R-LCO-Li-1173, and R-LCO-Li-1440; (d) EIS curves of S-LCO, R-LCO-Li-1173, and R-LCO-Li-1440; GITT curve of (e) S-LCO and (f) R-CO-Li-1440 as a function of time; (g) GITT curve of S-LCO and R-LCO-Li-1440 at the charging time; chemical diffusion coefficients of Li^+(D_{Li}^+) of (h) charging and (i) discharge.

S-LCO was weaker than that in R-LCO, indicating that the oxygen skeleton-layered structure of URM-LCO was repaired.

We investigated the effect of URM temperature on repairing the crystal structure of cathode materials using XRD, in which the reaction temperatures were determined by an infrared camera (Figure S10). The function of temperature with time during the URM process is plotted in Figure 3a. This process exhibited an ultrafast heating rate within one second, and the heating process was controlled to end after eight seconds. The repair temperature can be easily adjusted by the input current/voltage, which in our experiment corresponded to 1300, 1390, 1440, 1560, and 1700 K, respectively. Figure 3b shows that all the cathode materials regenerated by URM with Li_2CO_3 as the lithium source at different repair temperature possess a similar diffraction pattern, corresponding to the phase of a layered structure with the $R\bar{3}m$ space group. These samples are labeled as "R-LCO-Li-temperature" in Figure 3b. In contrast, for samples that underwent the same heat treatment without Li_2CO_3 lithium source (labeled as "R-LCO-temperature"), the additional peak at ~37° can be observed in the R-LCO-1300 and R-LCO-1390 samples, corresponding to the spinel Co_3O_4 (Figure 3c). However, the peak disappears with an increase of temperature in the other cathode materials, suggesting that the spinel Co_3O_4 is unstable at high temperature.

Next, we will discuss the electrochemical properties of the regenerated cathode under different URM conditions (reaction temperature and w/o Li supplement), which were evaluated in half cells via electrochemical impedance spectroscopy (EIS), battery cycling, and rate performance tests. As shown in Figure 3d, the rate capacity of all R-LCO with Li supplement at different rates increased with the temperature up to 1440 K and then decreased at higher temperatures. The R-LCO-Li-1440 exhibited the best rate capability among all the samples. The initial discharge capacity of the R-LCO-Li-1440 obtained at 0.1 C was as high as 133.0 mAh/g for (1 C = 147 mAh/g), while still maintaining a high value of 99.7 mAh/g at 4 C. The discharge capacities of R-LCO-Li-1440 were 133.0, 123.9, 119.6, 116.1, 109.9, and 99.6 mAh/g from 0.1 to 4 C (Figure S11), respectively, higher than those of the other samples repaired at all temperatures (Figure 3d). The corresponding voltage profiles of R-LCO-Li-1440 and R-LCO-1440 (without Li supplement at URM regeneration) at different charge/discharge rates are displayed in Figure 3e. In contrast, the R-LCO-1440 exhibits a comparably lower discharge capacity at all current densities. The EIS results of the different samples indicate that the R-LCO-Li-1440 exhibits the lowest interface impedance, which confirms its optimal rate performance (Figure 3f).

The long-term cycling performance of the R-LCO-Li-1440, R-LCO-1440, and S-LCO samples is presented in Figure 3g. During the cycling process, R-LCO-Li-1440 retained a stable discharge capacity at a relatively high level compared with R-LCO-1440 and S-LCO. After 300 cycles, the R-LCO-Li-1440 maintained a discharge capacity of 100.0 mAh/g, indicating its excellent cycling performance. In addition, the R-LCO samples via URM exhibit the best stability at 1440 K after 300 cycles (Figure S12), suggesting that this temperature is optimal for the repair process. Note the repair temperature in URM is higher than that in the conventional furnace-based method since the reaction time is significantly shorter. DFT calculations show that layered-structured LCO possesses lower free energy compared to spinel LCO at all temperatures, implying the former can endure high temperature for a short period.[49] According to the incremental capacity analysis (Figure 3h), the intensity of the discharge peak at 3.9 V in R-LCO-Li-1440 is higher than that in S-LCO, indicating lithium supplementation is essential during the repair process.

The electrochemical performance of LCO samples repaired by different annealing methods (URM at 1440 K, furnace annealing at 1173 K, which is the temperature commonly used

https://doi.org/10.1021/acsenergylett.3c00635
ACS Energy Lett. 2023, 8, 3005−3012

in conventional LCO repair process[50,51]) was investigated, as shown in Figure 4a,b. The S-LCO delivered a limited discharge capacity of 103.9 mAh/g, indicating it was in a Li-deficient state. In contrast, the R-LCO-Li-1440 exhibited an initial discharge capacity of 133.0 mAh/g, indicating that the URM efficiently realizes the lithium supplementation process. The furnace-annealed R-LCO-Li-1173 sample showed a discharge capacity of only 111.4 mAh/g, which was only slightly higher than that of S-LCO and R-LCO-1173. XRD analysis revealed the crystal structure of R-LCO-Li-1173 was repaired, while spinel Co_3O_4 was still present in the R-LCO-1173 (Figure S13). These results suggest that despite the long heat treatment, traditional heating processes may only repair cathode materials to a limited extent under the Ar atmosphere. The discharge capacity of R-LCO-1440 was also higher than that of R-LCO-1173, which is attributed to the short reaction time of the URM, which can avoid further lithium volatilization at high temperatures. We also conducted long-term cycling of R-LCO-Li-1173, R-LCO-Li-1440, and S-LCO; our results suggest that the R-LCO-Li-1440 exhibited better cycling stability and discharge capacity compared to R-LCO-Li-1173 (Figure 4c). EIS measurements of different samples were taken at the charged 4.3 V states. As shown in Figure 4d, R-LCO-Li-1440's charge transfer resistances (Rct) is lower than that of any other sample, indicating faster lithiation and delithiation kinetics. To investigate the kinetic characteristics of the S-LCO and R-LCO-Li-1440 electrode, we performed the galvanostatic intermittent titration technique (GITT) analysis from the third cycle and calculated the corresponding diffusion coefficients of Li^+ (D_{Li^+}) (Figure 4e-i). The calculated D_{Li^+} of R-LCO-Li-1440 is higher than that of S-LCO during charging and discharging, indicating that the cathode can be efficiently repaired by the URM. All of the above results suggest that the cathode materials repaired by the ultrafast method exhibit excellent electrochemical performance.

The ultrafast, roll-to-roll manufacturing of the regeneration process for cathode materials is envisioned using the schematic shown in Figure 5. During this process, a homogeneously

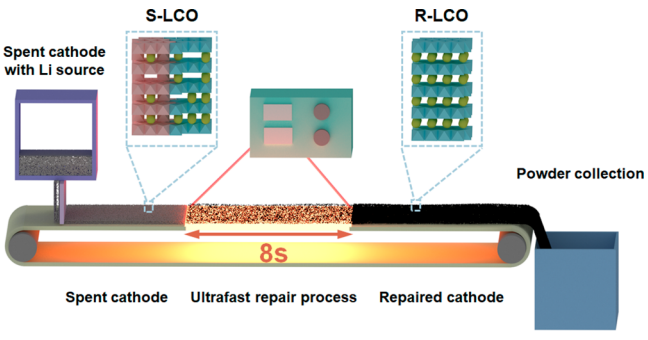

Figure 5. Schematic of roll-to-toll repair of cathode materials by the ultrafast repair method.

mixed precursor composed of the cathode material and lithium source continuously passes through the heating zone, allowing the cathode material to recover its original crystalline structure and electrochemical performance after rapid high-temperature treatment. This approach is made possible by the URM, making the ultrafast repair of cathode materials highly compatible with existing industrial protocols. This design offers great potential for ultrafast and efficient roll-to-roll regeneration of cathode materials.

In this Letter, we have demonstrated that spent LCO can be regenerated directly using an ultrafast repair method, taking only 8 s at the optimal reaction temperature of 1440 K. Systematic characterizations show that the phase structure of spent LCO can be completely restored to its original layered structure, and the electrochemical performance of repaired LCO is comparable to that of the pristine materials. The initial discharge capacity of optimized repaired LCO at 0.1 C is recovered to 133.0 mAh/g with an excellent cycle performance for more than 300 cycles. Furthermore, the repaired LCO exhibits superior rate capacity, which outperforms the furnace-repaired sample. This method is highly time- and energy-efficient, making it suitable for the practical direct regeneration of LCO cathodes for lithium-ion batteries. Our work on the ultrafast repair method opens up new avenues for the ultrafast and efficient repair of LIB cathode materials.

■ ASSOCIATED CONTENT

Supporting Information

The Supporting Information is available free of charge at https://pubs.acs.org/doi/10.1021/acsenergylett.3c00635.

Experimental section and supplementary figures, including SEM images, TEM images, elemental mapping result, Rietveld refinement of the XRD patterns, XPS patterns, temperature profile, and electrochemical performance (PDF)

■ AUTHOR INFORMATION

Corresponding Author

Jiayu Wan − *Department of Mechanical and Energy Engineering, Southern University of Science and Technology, Shenzhen 518055, China;* orcid.org/0000-0003-4603-3265; Email: wanjy@sustech.edu.cn

Authors

Yun-Chao Yin − *Department of Mechanical and Energy Engineering, Southern University of Science and Technology, Shenzhen 518055, China; Guangdong Research Center for Interfacial Engineering of Functional Materials, College of Materials Science and Engineering, Shenzhen University, Shenzhen 518060, China*

Chao Li − *Department of Mechanical and Energy Engineering, Southern University of Science and Technology, Shenzhen 518055, China;* orcid.org/0000-0002-5840-3633

Xueshan Hu − *Department of Mechanical and Energy Engineering, Southern University of Science and Technology, Shenzhen 518055, China*

Daxian Zuo − *Department of Mechanical and Energy Engineering, Southern University of Science and Technology, Shenzhen 518055, China*

Lin Yang − *Department of Mechanical and Energy Engineering, Southern University of Science and Technology, Shenzhen 518055, China*

Lihui Zhou − *Key Laboratory for Advanced Materials and Joint International Research Laboratory of Precision Chemistry and Molecular Engineering, Feringa Nobel Prize Scientist Joint Research Center, School of Chemistry and Molecular Engineering, East China University of Science and Technology, Shanghai 200237, China;* orcid.org/0000-0003-1434-8799

Jinlong Yang − *Guangdong Research Center for Interfacial Engineering of Functional Materials, College of Materials*

Science and Engineering, Shenzhen University, Shenzhen 518060, China; orcid.org/0000-0001-6065-7272

Complete contact information is available at: https://pubs.acs.org/10.1021/acsenergylett.3c00635

Author Contributions

#Y.-C.Y. and C.L. contributed equally to this work

Notes

The authors declare no competing financial interest.

■ ACKNOWLEDGMENTS

This work is funded by startup funding from Southern University of Science and Technology. We would like to express our gratitude to Mr. Weichen Sun, whose exceptional talent led to the design of the expressive cover that visually depicts the core idea of our work.

■ REFERENCES

(1) Natarajan, S.; Aravindan, V. Recycling Strategies for Spent Li-Ion Battery Mixed Cathodes. *ACS Energy Lett.* **2018**, *3* (9), 2101−2103.
(2) Bird, R.; Baum, Z. J.; Yu, X.; Ma, J. The Regulatory Environment for Lithium-Ion Battery Recycling. *ACS Energy Lett.* **2022**, *7* (2), 736−740.
(3) Lyu, Y.; Wu, X.; Wang, K.; Feng, Z.; Cheng, T.; Liu, Y.; Wang, M.; Chen, R.; Xu, L.; Zhou, J.; et al. An Overview on the Advances of $LiCoO_2$ Cathodes for Lithium-Ion Batteries. *Adv. Energy Mater.* **2021**, *11* (2), 2000982.
(4) Chu, S.; Cui, Y.; Liu, N. The path towards sustainable energy. *Nat. Mater.* **2017**, *16* (1), 16−22.
(5) Ciez, R. E.; Whitacre, J. F. Examining different recycling processes for lithium-ion batteries. *Nat. Sustain.* **2019**, *2* (2), 148−156.
(6) Gibb, B. C. The rise and rise of lithium. *Nat. Chem.* **2021**, *13* (2), 107−109.
(7) Nykvist, B.; Sprei, F.; Nilsson, M. Assessing the progress toward lower priced long range battery electric vehicles. *Energy Policy* **2019**, *124*, 144−155.
(8) Fan, E.; Li, L.; Wang, Z.; Lin, J.; Huang, Y.; Yao, Y.; Chen, R.; Wu, F. Sustainable Recycling Technology for Li-Ion Batteries and Beyond: Challenges and Future Prospects. *Chem. Rev.* **2020**, *120* (14), 7020−7063.
(9) Lai, X.; Huang, Y.; Gu, H.; Deng, C.; Han, X.; Feng, X.; Zheng, Y. Turning waste into wealth: A systematic review on echelon utilization and material recycling of retired lithium-ion batteries. *Energy Storage Mater.* **2021**, *40*, 96−123.
(10) Chen, M.; Ma, X.; Chen, B.; Arsenault, R.; Karlson, P.; Simon, N.; Wang, Y. Recycling End-of-Life Electric Vehicle Lithium-Ion Batteries. *Joule* **2019**, *3* (11), 2622−2646.
(11) Zhao, Y.; Fang, L.-Z.; Kang, Y.-Q.; Wang, L.; Zhou, Y.-N.; Liu, X.-Y.; Li, T.; Li, Y.-X.; Liang, Z.; Zhang, Z.-X.; et al. A novel three-step approach to separate cathode components for lithium-ion battery recycling. *Rare Metals* **2021**, *40* (6), 1431−1436.
(12) Kang, D. H. P.; Chen, M.; Ogunseitan, O. A. Potential Environmental and Human Health Impacts of Rechargeable Lithium Batteries in Electronic Waste. *Environ. Sci. Technol.* **2013**, *47* (10), 5495−5503.
(13) Winslow, K. M.; Laux, S. J.; Townsend, T. G. A review on the growing concern and potential management strategies of waste lithium-ion batteries. *Resour. Conserv. Recycl.* **2018**, *129*, 263−277.
(14) Mrozik, W.; Rajaeifar, M. A.; Heidrich, O.; Christensen, P. Environmental impacts, pollution sources and pathways of spent lithium-ion batteries. *Energy Environ. Sci.* **2021**, *14* (12), 6099−6121.
(15) Schmuch, R.; Wagner, R.; Hörpel, G.; Placke, T.; Winter, M. Performance and cost of materials for lithium-based rechargeable automotive batteries. *Nat. Energy* **2018**, *3* (4), 267−278.
(16) Lv, W.; Wang, Z.; Cao, H.; Sun, Y.; Zhang, Y.; Sun, Z. A Critical Review and Analysis on the Recycling of Spent Lithium-Ion Batteries. *ACS Sustainable Chem. Eng.* **2018**, *6* (2), 1504−1521.
(17) Zhang, X.; Li, L.; Fan, E.; Xue, Q.; Bian, Y.; Wu, F.; Chen, R. Toward sustainable and systematic recycling of spent rechargeable batteries. *Chem. Soc. Rev.* **2018**, *47* (19), 7239−7302.
(18) Piątek, J.; Afyon, S.; Budnyak, T. M.; Budnyk, S.; Sipponen, M. H.; Slabon, A. Sustainable Li-Ion Batteries: Chemistry and Recycling. *Adv. Energy Mater.* **2021**, *11* (43), 2003456.
(19) Baum, Z. J.; Bird, R. E.; Yu, X.; Ma, J. Lithium-Ion Battery Recycling−Overview of Techniques and Trends. *ACS Energy Lett.* **2022**, *7* (2), 712−719.
(20) Roy, J. J.; Rarotra, S.; Krikstolaityte, V.; Zhuoran, K. W.; Cindy, Y. D.-I.; Tan, X. Y.; Carboni, M.; Meyer, D.; Yan, Q.; Srinivasan, M. Green Recycling Methods to Treat Lithium-Ion Batteries E-Waste: A Circular Approach to Sustainability. *Adv. Mater.* **2022**, *34* (25), 2103346.
(21) Yao, Y.; Zhu, M.; Zhao, Z.; Tong, B.; Fan, Y.; Hua, Z. Hydrometallurgical Processes for Recycling Spent Lithium-Ion Batteries: A Critical Review. *ACS Sustainable Chem. Eng.* **2018**, *6* (11), 13611−13627.
(22) Garole, D. J.; Hossain, R.; Garole, V. J.; Sahajwalla, V.; Nerkar, J.; Dubal, D. P. Recycle, Recover and Repurpose Strategy of Spent Li-ion Batteries and Catalysts: Current Status and Future Opportunities. *ChemSusChem* **2020**, *13* (12), 3079−3100.
(23) Yang, X.; Zhang, Y.; Meng, Q.; Dong, P.; Ning, P.; Li, Q. Recovery of valuable metals from mixed spent lithium-ion batteries by multi-step directional precipitation. *RSC Adv.* **2021**, *11* (1), 268−277.
(24) Wang, T.; Yu, X.; Fan, M.; Meng, Q.; Xiao, Y.; Yin, Y.-X.; Li, H.; Guo, Y.-G. Direct regeneration of spent $LiFePO_4$ via a graphite prelithiation strategy. *Chem. Commun.* **2020**, *56* (2), 245−248.
(25) Guo, Y.; Guo, C.; Huang, P.; Han, Q.; Wang, F.; Zhang, H.; Liu, H.; Cao, Y.-C.; Yao, Y.; Huang, Y. Rejuvenating $LiNi_{0.5}Co_{0.2}Mn_{0.3}O_2$ cathode directly from battery scraps. *eScience* **2023**, *3*, 100091.
(26) Lin, J.; Chen, X.; Fan, E.; Zhang, X.; Chen, R.; Wu, F.; Li, L. A green repair pathway for spent spinel cathode material: coupled mechanochemistry and solid-phase reactions. *eScience* **2023**, 100110.
(27) Yang, Y.; Guo, J.-Z.; Gu, Z.-Y.; Sun, Z.-H.; Hou, B.-H.; Yang, A.-B.; Ning, Q.-L.; Li, W.-H.; Wu, X.-L. Effective Recycling of the Whole Cathode in Spent Lithium Ion Batteries: From the Widely Used Oxides to High-Energy/Stable Phosphates. *ACS Sustainable Chem. Eng.* **2019**, *7* (14), 12014−12022.
(28) Du, K.-D.; Meng, Y.-F.; Zhao, X.-X.; Wang, X.-T.; Luo, X.-X.; Zhang, W.; Wu, X.-L. A unique co-recovery strategy of cathode and anode from spent $LiFePO_4$ battery. *Sci. China-Mater.* **2022**, *65* (3), 637−645.
(29) Nie, H.; Xu, L.; Song, D.; Song, J.; Shi, X.; Wang, X.; Zhang, L.; Yuan, Z. $LiCoO_2$: recycling from spent batteries and regeneration with solid state synthesis. *Green Chem.* **2015**, *17* (2), 1276−1280.
(30) Wang, J.; Ma, J.; Jia, K.; Liang, Z.; Ji, G.; Zhao, Y.; Li, B.; Zhou, G.; Cheng, H.-M. Efficient Extraction of Lithium from Anode for Direct Regeneration of Cathode Materials of Spent Li-Ion Batteries. *ACS Energy Lett.* **2022**, *7* (8), 2816−2824.
(31) Shi, Y.; Zhang, M. H.; Meng, Y. S.; Chen, Z. Ambient-Pressure Relithiation of Degraded $Li_xNi_{0.5}Co_{0.2}Mn_{0.3}O_2$ ($0 < x < 1$) via Eutectic Solutions for Direct Regeneration of Lithium-Ion Battery Cathodes. *Adv. Energy Mater.* **2019**, *9* (20), 1900454.
(32) Ma, J.; Wang, J.; Jia, K.; Liang, Z.; Ji, G.; Zhuang, Z.; Zhou, G.; Cheng, H.-M. Adaptable Eutectic Salt for the Direct Recycling of Highly Degraded Layer Cathodes. *J. Am. Chem. Soc.* **2022**, *144* (44), 20306−20314.
(33) Wang, J.; Zhang, Q.; Sheng, J.; Liang, Z.; Ma, J.; Chen, Y.; Zhou, G.; Cheng, H.-M. Direct and green repairing of degraded $LiCoO_2$ for reuse in lithium- ion batteries. *Natl. Sci. Rev.* **2022**, *9* (8), nwac097.
(34) Wu, C.; Xu, M.; Zhang, C.; Ye, L.; Zhang, K.; Cong, H.; Zhuang, L.; Ai, X.; Yang, H.; Qian, J. Cost-effective recycling of spent

$LiMn_2O_4$ cathode via a chemical lithiation strategy. *Energy Storage Mater.* **2023**, *55*, 154−165.
(35) Park, K.; Yu, J. L.; Coyle, J.; Dai, Q.; Frisco, S.; Zhou, M.; Burrell, A. Direct Cathode Recycling of End-Of-Life Li-Ion Batteries Enabled by Redox Mediation. *ACS Sustainable Chem. Eng.* **2021**, *9* (24), 8214−8221.
(36) Wu, C.; Hu, J. M.; Ye, L.; Su, Z. P.; Fang, X. L.; Zhu, X. L.; Zhuang, L.; Ai, X. P.; Yang, H. X.; Qian, J. F. Direct Regeneration of Spent Li-Ion Battery Cathodes via Chemical Relithiation Reaction. *ACS Sustainable Chem. Eng.* **2021**, *9* (48), 16384−16393.
(37) Xu, P. P.; Yang, Z. Z.; Yu, X. L.; Holoubek, J.; Gao, H. P.; Li, M. Q.; Cai, G. R.; Bloom, I.; Liu, H. D.; Chen, Y.; et al. Design and Optimization of the Direct Recycling of Spent Li-Ion Battery Cathode Materials. *ACS Sustainable Chem. Eng.* **2021**, *9* (12), 4543−4553.
(38) Yu, X.; Yu, S.; Yang, Z.; Gao, H.; Xu, P.; Cai, G.; Rose, S.; Brooks, C.; Liu, P.; Chen, Z. Achieving low-temperature hydrothermal relithiation by redox mediation for direct recycling of spent lithium-ion battery cathodes. *Energy Storage Mater.* **2022**, *51*, 54−62.
(39) Gao, H. P.; Yan, Q. Z.; Xu, P. P.; Liu, H. D.; Li, M. Q.; Liu, P.; Luo, J.; Chen, Z. Efficient Direct Recycling of Degraded $LiMn_2O_4$ Cathodes by One-Step Hydrothermal Relithiation. *ACS Appl. Mater. Interfaces* **2020**, *12* (46), 51546−51554.
(40) Fan, M.; Meng, Q.; Chang, X.; Gu, C.-F.; Meng, X.-H.; Yin, Y.-X.; Li, H.; Wan, L.-J.; Guo, Y.-G. In Situ Electrochemical Regeneration of Degraded $LiFePO_4$ Electrode with Functionalized Prelithiation Separator. *Adv. Energy Mater.* **2022**, *12* (18), 2103630.
(41) Peng, D.; Wang, X.; Wang, S.; Zhang, B.; Lu, X.; Hu, W.; Zou, J.; Li, P.; Wen, Y.; Zhang, J. Efficient regeneration of retired $LiFePO_4$ cathode by combining spontaneous and electrically driven processes. *Green Chem.* **2022**, *24* (11), 4544−4556.
(42) Chen, Y.; Egan, G. C.; Wan, J.; Zhu, S.; Jacob, R. J.; Zhou, W.; Dai, J.; Wang, Y.; Danner, V. A.; Yao, Y.; et al. Ultra-fast self-assembly and stabilization of reactive nanoparticles in reduced graphene oxide films. *Nat. Commun.* **2016**, *7* (1), 12332.
(43) Wang, C.; Ping, W.; Bai, Q.; Cui, H.; Hensleigh, R.; Wang, R.; Brozena, A. H.; Xu, Z.; Dai, J.; Pei, Y.; et al. A general method to synthesize and sinter bulk ceramics in seconds. *Science* **2020**, *368* (6490), 521−526.
(44) Hu, X.; Zuo, D.; Cheng, S.; Chen, S.; Liu, Y.; Bao, W.; Deng, S.; Harris, S. J.; Wan, J. Ultrafast materials synthesis and manufacturing techniques for emerging energy and environmental applications. *Chem. Soc. Rev.* **2023**, *52* (3), 1103−1128.
(45) Dong, Q.; Li, T.; Yao, Y.; Wang, X.; He, S.; Li, J.; Luo, J.; Zhang, H.; Pei, Y.; Zheng, C.; et al. A General Method for Regenerating Catalytic Electrodes. *Joule* **2020**, *4* (11), 2374−2386.
(46) Wang, C.; Xie, H.; Ping, W.; Dai, J.; Feng, G.; Yao, Y.; He, S.; Weaver, J.; Wang, H.; Gaskell, K.; et al. A general, highly efficient, high temperature thermal pulse toward high performance solid state electrolyte. *Energy Storage Mater.* **2019**, *17*, 234−241.
(47) Zhang, L.; Xu, Z.; He, Z. Electrochemical Relithiation for Direct Regeneration of $LiCoO_2$ Materials from Spent Lithium-Ion Battery Electrodes. *ACS Sustainable Chem. Eng.* **2020**, *8* (31), 11596−11605.
(48) Zhou, S.; Fei, Z.; Meng, Q.; Dong, P.; Zhang, Y.; Zhang, M. Collaborative Regeneration of Structural Evolution for High-Performance of $LiCoO_2$ Materials from Spent Lithium-Ion Batteries. *ACS Appl. Energy Mater.* **2021**, *4* (11), 12677−12687.
(49) Kim, S.; Hegde, V. I.; Yao, Z.; Lu, Z.; Amsler, M.; He, J.; Hao, S.; Croy, J. R.; Lee, E.; Thackeray, M. M.; et al. First-Principles Study of Lithium Cobalt Spinel Oxides: Correlating Structure and Electrochemistry. *ACS Appl. Mater. Interfaces* **2018**, *10* (16), 13479−13490.
(50) Mizushima, K.; Jones, P. C.; Wiseman, P. J.; Goodenough, J. B. Li_xCoO_2 ($0 < x < -1$): A new cathode material for batteries of high energy density. *Mater. Res. Bull.* **1980**, *15* (6), 783−789.
(51) Zhang, J.-N.; Li, Q.; Ouyang, C.; Yu, X.; Ge, M.; Huang, X.; Hu, E.; Ma, C.; Li, S.; Xiao, R.; et al. Trace doping of multiple elements enables stable battery cycling of $LiCoO_2$ at 4.6 V. *Nat. Energy* **2019**, *4* (7), 594−603.

https://doi.org/10.1021/acsenergylett.3c00635
ACS Energy Lett. 2023, 8, 3005−3012